Proceedings of the
Annual Stability Conference
Structural Stability Research Council
Baltimore, Maryland, April 10-13, 2018

Flexural resistance of longitudinally stiffened curved I-girders

Lakshmi P. Subramanian[1], Donald W. White[2]

Abstract
The current AASHTO Specifications neglect the contribution of the longitudinal stiffeners to the flexural resistance of slender-web I-girders after the webs have undergone bend-buckling. The authors have previously developed a cross-section model to address this conservatism, and proposed a simplified equation to calculate the web bend-buckling factor R_b for straight longitudinally stiffened I-girders. The recommendations are shown to work well not only for the yield limit state, but also for members with lateral torsional buckling and flange local buckling as the controlling limit states. The model also works well for cases with high moment and high shear. Horizontally-curved girders experience larger flange lateral bending stresses due to curvature, and the Specifications treat the compression flanges of such members as equivalent beam-columns. The current paper examines whether the proposed modified equations for R_b developed based on straight longitudinally stiffened girders can be applied to horizontally curved longitudinally stiffened I-girders within the framework of the current beam-column type equations (termed as the 1/3rd rule). The paper first illustrates that the design of curved longitudinally stiffened girders is always limited to either the yield limit state or the shorter lengths in the inelastic LTB region. The paper also recommends an increase in the curvature parameter, Z from the current value of 10 to 13 using finite element simulations on homogeneous I-girders subjected to uniform moment.

1. Introduction

The AASHTO (2016) provisions stipulate that flange lateral bending effects due to curvature must be considered for discretely braced flanges in horizontally curved girders, i.e., the Specifications require that compression flanges of curved girders have sufficient strength with respect to lateral torsional buckling (LTB), and flange local buckling (FLB) limit states while including the consideration of flange lateral bending. The flange lateral bending effects are considered by means of a "beam-column" type equation termed as the 1/3rd rule.

The one-third rule, expressed in terms of the flange stresses computed from an elastic analysis, is given by AASHTO Equation 6.10.8.1.1-1

$$f_{bu} + \frac{1}{3} f_l \le \phi_f F_{nc} \tag{1}$$

[1] Assistant Professor, Indian Institute of Technology Madras, India, <lakshmipriya@iitm.ac.in>
[2] Professor, Georgia Institute of Technology, <dwhite@gatech.edu>

where, f_{bu} is the compression flange stress due to major-axis bending (analogous to a beam-column axial load), f_l is the maximum second-order flange lateral bending stress within the unbraced length (analogous to the bending moment within an equivalent beam-column member), ϕ_f is the AASHTO resistance factor for flexure, and F_{nc} is the nominal flexural resistance of the flange for major-axis bending. The 1/3 factor provides a linear approximation of the equivalent beam-column resistance of the compression flange, accurate for $f_l \leq 0.6F_{yf}$, where F_{yf} is the yield strength of the flange (White and Grubb 2005). White et al. (2001) show that, of various options studied, the one-third rule gives the best correlation with strength data from experimental tests as well as results from extensive FEA parametric studies.

The one-third rule equation is limited to I-sections loaded predominantly in major-axis bending. In the event that f_l exceeds $0.6F_{yf}$, the reduction in the major-axis bending resistance due to flange lateral bending may be greater than that represented by Eq. (1). The one-third rule is recommended for use only when the following limits are satisfied (White and Grubb 2005; White et al. 2001):

1. The flange lateral bending stress, $f_l \leq 0.6F_{yc}$ (F_{yc} is the yield strength of the compression flange)
2. The flange width-to-thickness ratio, $b/t_f \leq 24$.
3. The ratio of the unbraced length to the radius of curvature, $L_b/R \leq 0.1$.
4. The member unbraced length, $L_b \leq L_r$, where L_r is the limiting effective unbraced length beyond which the compression flange strength under uniform bending is characterized by the theoretical elastic lateral torsional buckling resistance.

The original development of the one-third rule (White et al. 2001) did not address curved I-girders with web longitudinal stiffeners. The research presented in this paper assesses the applicability of the 1/3rd rule for these member types, while constraining the cross-section and member geometry to satisfy the above four parameters used in the development of the 1/3rd rule.

The authors have previously developed a cross-section model and a simplified equation for the web bend-buckling factor R_b for straight longitudinally stiffened girders (Subramanian and White 2017a; 2017b). In addition, the authors have recommended modified expressions to assess the LTB resistance of longitudinally stiffened girders (Subramanian and White 2017c). These recommendations are briefly discussed below:

1.1 Proposed equation to calculate R_b for straight longitudinally-stiffened girders

The web bend-buckling factor from the cross-section model proposed in (Subramanian and White 2017a) is approximated by

$$R_{bPr} = 1.07 - 0.12\frac{D_c}{D} - \frac{a_{wc}}{1200 + 300a_{wc}}\left[\frac{D}{t_w} - \lambda_{rwD}\right] \leq 1.0 \tag{2}$$

where:

For homogeneous longitudinally stiffened girders,

$$\lambda_{rwD} = 0.95\sqrt{\frac{Ek}{F_{yc}}} \tag{3}$$

For hybrid longitudinally stiffened girders with one change in grade of steel between one or both flanges and the longitudinal stiffener,

$$\lambda_{rwD} = \left(\frac{1}{2D_c / D}\right)5.7\sqrt{\frac{E}{F_{yc}}} \tag{4}$$

The term $0.95\sqrt{Ek/F_{yc}}$ in Eq. (3) is the limit on D/t_w at which elastic web bend buckling theoretically occurs at a compression flange stress equal to F_{yc}. Therefore, this term is effectively the noncompact limit of a longitudinally stiffened web in homogeneous girders, written in terms of the total web depth D. The term a_{wc} is the ratio of two times the web area in compression to the area of the compression flange, and k is the bend buckling coefficient, defined in AASHTO LRFD Article 6.10.1.9.2. In the above equations, D_c is calculated on the gross cross-section including the contribution of the longitudinal stiffener. Subramanian and White (2017b) explain that when the stiffener depth d_s is increased to $0.758D_c$ or larger, the longitudinal stiffener is essentially ineffective in restraining web bend buckling (based on AASHTO LRFD Article 6.10.1.9.2). As such, for $d_s \geq 0.758D_c$, the longitudinally stiffened homogeneous girder noncompact web limit, λ_{rwD} (expressed in terms of D/t_w), is equivalent to the noncompact web limit for a non-longitudinally stiffened web, $\lambda_{rwDc} = 137$ (expressed in terms of the web slenderness $2D_c/t_w$). That is, for $d_s \geq 0.758D_c$, $\lambda_{rwD} = \lambda_{rwDc}\,(D/D_c)$.

When Eqs. (2) and (4) are employed for hybrid girders, the resulting R_{bPr} (Proposed R_b) is to be combined multiplicatively with the traditional hybrid factor R_h to determine the girder "plateau" strength in major-axis bending, similar to the calculations for non-longitudinally stiffened girders (Subramanian and White 2017b).

1.2 Proposed recommendations to calculate LTB resistance of longitudinally-stiffened girders

- The LTB plateau length is recommended as $L_p = 0.63 r_t \sqrt{E/F_y}$.
- The maximum stress level for elastic LTB, F_{yr}, is calculated as the smaller of the web bend-buckling stress, F_{crw}, and $0.5F_{yc}$. The bend-buckling stress of the longitudinally stiffened web, F_{crw}, is calculated using the AASHTO LRFD Article 6.10.1.9 provisions.
- If F_{crw} is smaller than $F_{yr} = 0.5F_{yc}$, the inelastic LTB resistance of the longitudinally stiffened girder is determined by linearly interpolating between the plateau strength at $KL_b = L_p$, i.e., the point (L_p, $R_{bPr}F_{yc}$), and the point (L_1, F_{crw}). The term L_1 is the effective unbraced length at which the elastic LTB stress F_{nc} is equal to F_{crw}. Conversely, if F_{crw} is greater than $F_{yr} = 0.5F_{yc}$, the inelastic LTB resistance is obtained by linearly interpolating between (L_p, $R_{bPr}F_{yc}$) and (L_r, $0.5F_{yc}$), where L_r is defined here as the length at which the theoretical elastic LTB strength is equal to $F_{yr} = 0.5F_{yc}$. (It should be noted that the current AASHTO provisions define L_r as the length corresponding to $F_{yr} = 0.7F_{yc}$ for homogeneous slender-web I-girders.)
- For unbraced lengths larger than the length corresponding to a theoretical elastic LTB compression flange stress level equal to min (F_{crw}, $0.5F_{yc}$), i.e., for unbraced lengths larger than max (L_1, L_r), the elastic LTB equation of the current AASHTO Specifications, with $R_b = 1$, is used to determine the LTB resistance.
  In this paper, L_p, L_r and F_{yr} refer to the corresponding quantities calculated using the proposed LTB equations.

The principal objective of this paper is to assess whether the above recommendations on R_b and LTB resistance computations for straight longitudinally stiffened girders may be used along with the existing 1/3rd rule in AASHTO. These recommendations will be used to compute the right-hand side, F_{nc} in Eq. (1).

In developing the cross-section and member parameters for analysis, it is found that the design space of curved longitudinally stiffened girders is limited to the LTB plateau and the shorter lengths in the inelastic LTB region. This is discussed in the following section.

2. Design Space of Curved Longitudinally Stiffened Girders

This section reviews the AASHTO (2016) requirements for the design of curved girders and shows that the Specification requirements are such that curved longitudinally stiffened I-girders can only be designed with unbraced lengths in the plateau and shorter inelastic buckling ranges of the LTB strength curve.

The following discussions focus on the strength of curved I-girders in the bridge final constructed condition. It is assumed that the stability of the overall bridge structural system is ensured by the satisfaction of the AASHTO LRFD design rules, and as such, the bridge system provides lateral and/or torsional restraint at the ends of the girder unbraced lengths. Stability of the individual girders and units during lifting and erection, and stability of the partially erected structure during construction are not addressed in this paper.

2.1 Design Limits in AASHTO LRFD Specifications

The following design limits are stipulated by the AASHTO LRFD Specifications:

1. Cross-frame spacing

   The maximum spacing of cross-frames and diaphragms in horizontally curved I-girder bridges is specified in AASHTO Eq. 6.7.4.2-1 as

   $$L_b \le L_r \tag{5}$$

   and

   $$L_b \le R/10 \tag{6}$$

   where, L_b is the cross-frame spacing, L_r is the limiting unbraced length beyond which the member resistance is governed by elastic lateral torsional buckling, and R is the minimum radius of curvature of the girder. In addition to limiting the cross-frame spacing to the smaller of L_r and $R/10$, AASHTO Article 6.7.4.2 limits the spacing to

   $$L_b \le 30 \text{ ft.} \tag{7}$$

   Equation (6) is a practical upper-bound for the subtended angle between cross-frames, although there is limited data that demonstrates the validity of the one-third rule for members with $L_b/R > 0.2$ (White et al. 2001).

2. Flange width-to-thickness ratio.

   The AASHTO LRFD Specifications restrict $b_f/2t_f$ to 12 (AASHTO Eq. 6.10.2.2-1). This restriction is imposed to ensure that that flange does not distort excessively when welded to the web. This limit also effectively precludes the use of slender flanges in bridge I-girders.

3. Ratio of web depth to flange width.

   The AASHTO LRFD Specifications limit the ratio D/b_f to 6 (AASHTO Eq. 6.10.2.2-2). This limit on both flanges allows stiffened interior web panels to develop postbuckling shear resistance due to tension-field action under certain conditions (if the dimensions also satisfy AASHTO Eq. 6.10.9.3.2-1, which addresses the ratio of the area of the flanges to the area of the girder web). I-girders with D/b_f close to the above limit are inefficient with respect to flange lateral bending. As such, smaller D/b_f values are advisable for most curved bridges. The D/b_f limit of 6 can be appropriate particularly for longer-span straight I-girders however. This

is because, given the typical 25 to 30 ft maximum cross-frame spacing, the most economical designs for these types of bridges will have relatively narrow flanges compared to the section depth. In the following developments, the AASHTO LRFD limit on D/b_f is employed to evaluate the bounds on curved girder responses.

4. Ratio of flange thickness to web thickness.
   AASHTO LRFD Article 6.10.2.2 stipulates that the ratio of t_f/t_w must be greater than or equal to 1.1. This requirement is intended to ensure adequate restraint of web shear buckling by the flange, among other factors. In addition, a minimum web thickness, t_w, of 0.5 inches is commonly used in bridge I-girder construction, although this limit is not specified explicitly in the AASHTO LRFD Specifications.
5. Ratio of moment of inertia of the compression flange to that of the tension flange, taken about a vertical axis in the plane of the web.
   AASHTO LRFD Article 6.10.2.2 also stipulates that the ratio I_{yc}/I_{yt} must be within the limits of 0.1 and 10. Cross-sections outside of these limits are extremely singly-symmetric, and pose several problems with regard to constructability and applicability of the design equations.
6. Panel aspect ratio.
   AASHTO LRFD Article 6.10.9.1 restricts the ratio of the transverse stiffener spacing-to-web-depth to 1.5 in longitudinally stiffened girders. It should be noted that generally the connection plates at the cross-frame locations act as transverse stiffeners.
7. Longitudinal stiffener sizing requirements.
   AASHTO Article 6.10.11.3.3 lists the lateral rigidity and radius of gyration requirements on longitudinal stiffeners. These are discussed in detail for straight I-girders in (Subramanian and White 2017d). While the radius of gyration requirement on the longitudinal stiffener is the same for horizontally curved and straight girders, the AASHTO Specifications multiply the required stiffener lateral moment of inertia by a curvature correction factor, β, as indicated in AASHTO Eq. 6.10.11.3.3-1:

$$I_l \geq Dt_w^3\left[2.4\left(\frac{d_o}{D}\right)^2 - 0.13\right]\beta \tag{8}$$

   Curved webs tend to bow more than straight webs; therefore, the rigidity requirement for longitudinal stiffeners on curved webs is larger than that for straight webs. The curvature correction factor addresses this behavior and is calculated using AASHTO Eqs. 6.10.11.3.3-3 and 6.10.11.3.3-4:

$$\beta = \frac{Z}{6} + 1 \tag{9}$$

   for members with the longitudinal stiffener on the side of the web opposite from the center of curvature, and

$$\beta = \frac{Z}{12} + 1 \tag{10}$$

   for members with the longitudinal stiffener on the side of the web toward the center of curvature. In these equations, Z is the curvature parameter defined below.
8. Curvature Parameter, Z.
   The curvature parameter, Z is given by AASHTO Eq. 6.10.11.3.3-5:

$$Z = \frac{0.95d_o^2}{Rt_w} \leq 10 \tag{11}$$

For straight I-girders Z is zero, and hence β in Eqs.(8) through (10) is equal to 1.0. This research aims to evaluate if the current limit of 10 on Z may be potentially increased.

The parameters and limits discussed in this Section are interdependent. These interdependencies influence the range of possible longitudinally stiffened I-girder designs. In general, I-section member strengths tend to be size independent, i.e. if the non-dimensional parameters (such as D/t_w, D/b_{fc}, etc.) are held constant, and a girder is simply scaled in size, the flexural resistance as a fraction of M_{yc} is unchanged. However, the design limits imposed in AASHTO, particularly on the maximum unbraced length (L_b = 30 ft) cause the extent of the unbraced lengths encountered for longitudinally stiffened girders (relative to L_p and L_r) to be size dependent.

2.2 Estimation of Flange Lateral Bending Stresses

In lieu of a refined analysis, AASHTO (2016) permits the use of the equation

$$M_{lat} = \frac{ML_b^2}{NRD} \tag{12}$$

to estimate the first-order lateral bending moment in I-girder flanges due to horizontal curvature. In this equation, M_{lat} is the flange lateral bending moment, M is the major-axis bending moment, L_b is the unbraced length, R is the girder radius, D is the girder web depth, and N is a constant, taken as 12 in this paper. The first-order compression flange lateral bending stress, f_{l1} may be calculated by dividing M_{lat} by the elastic section modulus of the compression flange:

$$f_{l1} = \frac{ML_b^2}{NRD\left(b_{fc}^2 t_f / 6\right)} = \frac{6M}{NDb_{fc}t_f}\left(\frac{L_b}{R}\right)\left(\frac{L_b}{b_{fc}}\right) \tag{13}$$

The second-order flange lateral bending stresses by amplifying the first-order stresses f_{l1} using

$$f_l = \left(\frac{0.85}{1-\frac{f_{bu}}{F_{cr}}}\right) f_{l1} \geq f_{l1} \tag{14}$$

where the term F_{cr} is the elastic lateral buckling stress of the flange under consideration, calculated from the theoretical elastic LTB equation. However, unlike in the LTB calculations, this stress is not limited to the LTB plateau strength. The amplification factor in Eq. (14) tends to be significantly conservative for larger unsupported lengths, where f_{bu} approaches F_{cr}. Refined nonlinear analysis as described in Section 3.4 more accurately captures second-order effects.

2.3 Effective Length Factor for Curved I-Girders

This paper focusses on I-girders in their final constructed condition, where the cross-frames provide lateral and/or torsional restraint to the girders at each end of their unbraced lengths, L_b. Given these conditions, various researchers, e.g., Simpson (2000) and White et al. (2001), have observed that the critical interior unbraced lengths of curved girder compression flanges tend to fail laterally in a manner in which they deflect outwards similar to the behavior of a fixed-fixed beam subjected to a distributed lateral load. White et al. (2001) considered various test setups and showed that warping and lateral bending restraints are developed in curved members at the cross-frame locations due to continuity with adjacent unbraced segments, and that these restraints result in near zero incremental flange lateral bending rotations, along with significant flange lateral bending moments at the ends of the unbraced segments, as the strength condition is approached.

White et al. (2001) suggested that when $L_b/R < 0.05$, the actual unsupported length should be used in calculating the amplification of the flange lateral bending stresses and in calculating the base lateral torsional buckling resistance; however, they suggested the use of $K = 0.5$ in all cases when $L_b/R > 0.05$. Similarly, any critical *end* unbraced lengths in typical curved I-girders tend to behave much like propped cantilevers as the lateral stability limit is approached, such that $KL_b = 0.7L_b$ would be the best estimate within these segments.
In the current paper, the authors have used a simpler curved I-girder test setup compared to those utilized by White et al. (2001). This setup, discussed in Section 3.2, has physically fixed conditions at the ends of the test specimens, and thus directly yields an LTB effective length factor of 0.5.

2.4 Practical Limits on Design of Curved Longitudinally Stiffened I-Girders
This section shows how curved longitudinally stiffened I-girders are necessarily restricted to unbraced lengths that fall within the plateau and shorter inelastic buckling ranges of the LTB strength curve by the various stipulations in AASHTO LRFD discussed in Section 2.1. The example cross-sections considered in this section are doubly-symmetric homogeneous slender-web I-sections. The yield strength considered is 50 ksi. The web thickness t_w is taken as a constant value of 0.5 in. The following girder parameters are considered:

1. D/t_w = 150, 200, 250 and 300, or D = 75 in. (6.25 ft), 100 in. (8.33 ft), 125 in. (10.41 ft) and 150 in. (12.5 ft) given the web thickness of 0.5 in;
2. D/b_f = 2, 3, 4, 5 and 6;
3. $b_f/2t_f$ = 6, 7, 8, 9, 10 and 12;
4. L_b/R = 0.05, 0.075 and 0.1.

The girder dimensions are minimized by the use of the minimum practical web thickness (0.5 in) in combination with other non-dimensional design parameters listed above. This means that limits other than Eq. (7) are more apt to control the design. Longitudinally stiffened girders with larger web thicknesses would tend to be more restricted by Eq. (7), leading to girder designs being restricted to the plateau and shorter lengths within the inelastic region of the LTB strength curve. The flange widths are determined from the selected D/b_f values, and the flange thicknesses are determined given the specified values of $b_f/2t_f$. For the cases with relatively wide and stocky flanges, the flange thicknesses can exceed 4 in. These cases are eliminated from further consideration. For instance, a girder with D/t_w = 300, D/b_f = 3, and $b_f/2t_f$ = 6 would have a flange thickness of 4.2 in. As such, this girder is eliminated from consideration. From the girder web depths, selected based on the minimum t_w = 0.5 in. and the specified range of D/t_w values, one can gain a rough perspective of the types of bridge span lengths involved if we assume a representative arc span length to girder depth L_{as}/D of 25. The associated bridge arc span lengths are L_{as} = 156, 208, 260 and 312 ft for D = 75, 100, 125 and 150 in.

Given these cross-section parameters, the maximum unbraced length that can be employed for any given cross-section is determined in this study via an iterative process, ensuring that the stresses at the strength limit state are such that the one-third rule in Eq. (1) is satisfied. The iteration is carried out in the following manner:

1. The unbraced length is first set at 30 ft, and f_{bu} is computed such that Eq. (1) is satisfied exactly.
2. In this calculation, f_l is expressed as a function of f_{bu} based on Eqs. (13) and (14) (In these equations, $M = f_{bu} S_{xc}$, where S_{xc} is the elastic section modulus of the cross-section including the longitudinal stiffener).

3. The member strength F_{nc} is calculated using R_{bPr} from Eq. (2).
4. If the above unbraced lengths result in a value of f_l larger than $0.6F_{yf}$, then the unbraced length smaller than 30 ft that makes f_l exactly equal to $0.6F_{yf}$ is determined.

It is found that the L_b = 30 ft limit controls for sections with wider flanges and larger depths, while the limit on f_l controls for cross-sections having narrower flanges and smaller depths. The effective length factor is taken as 0.5 when calculating the amplification factor for the flange lateral bending stresses, and when determining F_{nc} from the LTB strength equations.

The size of the longitudinal stiffener is sensitive to d_o/D, d_o/R and D/t_w via Eqs. (8) through (10). The longitudinal stiffener is sized by satisfying Eq. (8), as well as satisfying the maximum width to thickness limit based on AASHTO Eq. 6.10.11.3.2-1. This approach effectively gives the smallest area of the longitudinal stiffener that meets the AASHTO LRFD requirements, given a selected stiffener spacing d_o. Further, the stiffener is located on the side of the web opposite from the center of curvature and at the theoretical optimum depth for flexure, $0.4D_{cg}$ from the compression flange in this section. (D_{cg} denotes the depth of web in compression for the gross cross-section, measured from the inside of the compression flange, including the influence of the longitudinal stiffener on the gross cross-section properties.) The AASHTO Eq. (6.10.11.3.3-2) requirement on the radius of gyration of the longitudinal stiffener does not control for any of the homogeneous girder designs considered in this paper.

Although the subsequent studies in this paper evaluate the potential of increasing the maximum limit on Z, $Z \leq 10$ is used in creating the example girder designs in the study presented in this section. In addition, d_o is selected such that $d_o \leq 2D$ and $d_o \leq L_b$. A maximum limit of $d_o = 2D$ is chosen in this paper, as the authors have previously recommended an increase in the current transverse stiffener spacing limit of $1.5D$ (Subramanian and White 2017a).
Given the above complexities, and recognizing that the girder unbraced length required to satisfy $L_b \leq 30$ ft and $f_l \leq 0.6F_{yf}$ is not sensitive to the longitudinal stiffener size, it was decided to determine the value of $d_o \leq 2D$ and $\leq L_b$ that restricts Z (Eq. 11) to a maximum of 10 by a rough estimate. In addition to using this estimated value of d_o, it was decided to assume $Z = 10$ in determining a longitudinal stiffener size via Eq. (11). Once the longitudinal stiffener was sized, the above iterative procedure was employed to determine the maximum limit on L_b; the radius of curvature, R, was determined given the specified L_b/R values, and the adherence to $Z \leq 10$ and $d_o \leq L_b$ was checked. Girders with $KL_b/D < 1$ (i.e., $L_b/D < 2$) were omitted from consideration, since these unbraced lengths are so small such that the designs verge on being impractical. The resulting designs have Z values ranging from 5.5 to 10.0. Also, d_o is less than or equal to the $2D$ limit specified in the proposed provisions (Subramanian and White 2017d).

It is important to note that this section is focused on determining the LTB design range (i.e., the maximum possible values of KL_b/L_p) for curved longitudinally stiffened I-girders. The parameters Z and d_o/D affect the size of the longitudinal stiffener, and the size of the longitudinal stiffener affects the elastic section modulus of the cross-section, the LTB radius of gyration (r_t) and the value of R_{bPr} for the cross-section. This in turn affects the cross-section design strength (F_{nc}), which is used in determining the maximum unbraced length for the girder. However, the parameters Z and d_o/D, and ultimately the longitudinal stiffener size, do not affect the values of KL_b/L_p significantly. Furthermore, although the curvature parameter Z is restricted to 10 in determining

the limits on KL_b/L_p in this study, results for test simulations with Z up to 13 are considered in Section 3.4.

A full matrix of the above cross-sectional parameters yields a total of 360 different cross-sections. These cross-sections include girders with both compact and noncompact flanges (girders with $b_{fc}/2t_{fc}$ of 10, 12 are noncompact-flange sections for F_{yf} = 50 ksi). The unbraced length-to-depth (L_b/D) values range from:

1. 4.80 for girders with D/t_w = 150, the widest flanges and L_b/R = 0.05, to
2. 1.22 for a girder with D/t_w = 150, the most-narrow and most-slender flanges (smallest flange area), and largest curvature L_b/R = 0.1.

The unbraced length-to-flange width (L_b/b_f) values range from:

1. 4.80 for girders with D/t_w = 300, the widest flanges, and L_b/R = 0.1, to
2. 22.7 for a girder with D/t_w = 150, D/b_f = 6, $b_f/2t_f$ = 6 and L_b/R = 0.05.

As noted above, test girders with $KL_b/D < 1$ ($L_b/D < 2$) are eliminated from consideration. It is emphasized that L_p in these discussions is the limiting unbraced length for the LTB "plateau" resistance given by the *proposed* equations, using the coefficient 0.63 (see Section 1.2). The values for KL_b/L_p based on the current AASHTO equations are even smaller. It is observed that the parameter $b_{fc}/2t_{fc}$ has, at best, a minor influence on the maximum unbraced length a girder can achieve. The upper limit on the maximum L_b of 30 ft governs with the exception of girders with larger D/b_f values, and the maximum $L_b < 30$ ft is more sensitive to the flange width than the flange thickness for the narrow flange sections. However, narrow flanges with the smallest values of $b_{fc}/2t_{fc}$ result in the smallest values of L_p, and hence, the largest values of KL_b/L_p. As noted above, girders with KL_b smaller than the girder web depth ($L_b/D \leq 2$), are omitted from the discussions. This condition occurs predominantly when the flanges are narrow (D/b_{fc} = 5 and 6), the radius of curvature is large (L_b/R = 0.075 and 0.1), and D is smaller than 300 (i.e., D = 75, 100 and 125 in., which is derived from D/t_w = 150, 200 and 250, given t_w = 0.5 in.).

The following sub-section discusses the maximum potential KL_b/L_p values as determined from the above AASHTO design constraints and limits on the associated flange lateral bending stresses. It is determined that the parameters D, D/b_{fc} and L_b/R have the greatest influence on the flange lateral bending stresses, as well as on the maximum unbraced lengths for which the girders can be designed.

The maximum KL_b/L_p values that satisfy the AASHTO LRFD constraints vary in large part as a function of the web depth, D, the web depth to flange width ratio, D/b_f, and the subtended angle between the cross-frame locations, L_b/R. Figures 1 and 2 show the maximum limits on KL_b/L_p as a function of these parameters for all the girders considered in this study. Figure 1 shows the data for girders where the cross-frame spacing is controlled by the maximum allowed value of L_b = 30 ft. Figure 2 shows the data for those girders where the cross-frame spacing is less than 30 ft, i.e., where the design is controlled by the maximum allowable flange lateral bending stress of $0.6F_y$.

The following can be gleaned from Figs. 1 and 2:

1. When $L_b/R \leq 0.05$, the larger depth girders (D = 10.4 ft and 12.5 ft) always can be designed using L_b = 30 ft (i.e., the limit $f_l \leq 0.6F_y$ is not violated for any of these girders), even when the

girders have the most-narrow flanges ($D/b_f = 6$). By inference, this observation would also apply to any girders of larger depth.

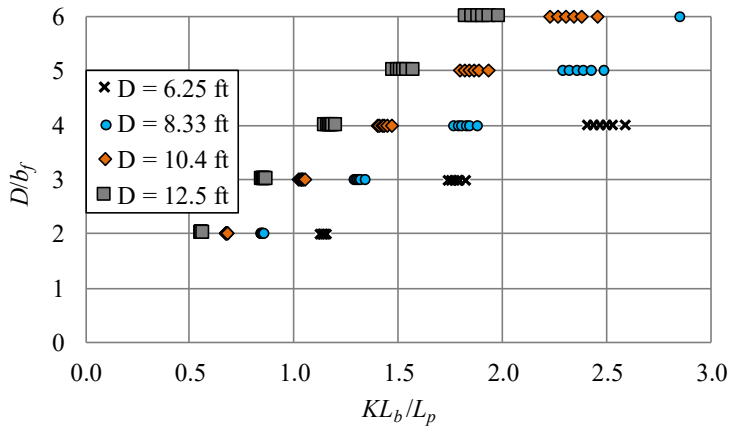

(a) $L_b/R = 0.05$

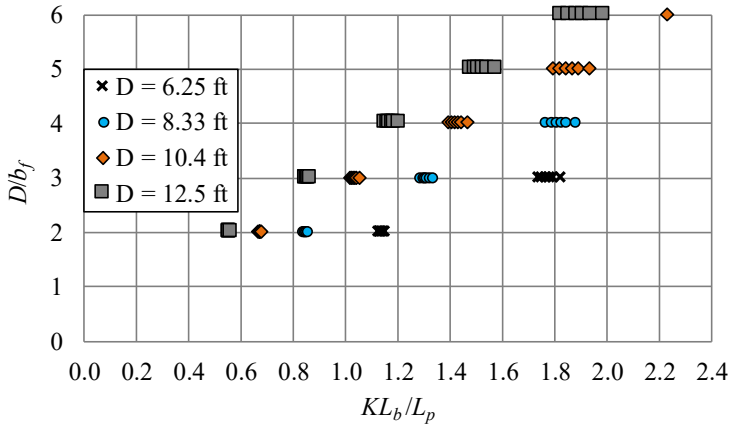

(b) $L_b/R = 0.075$

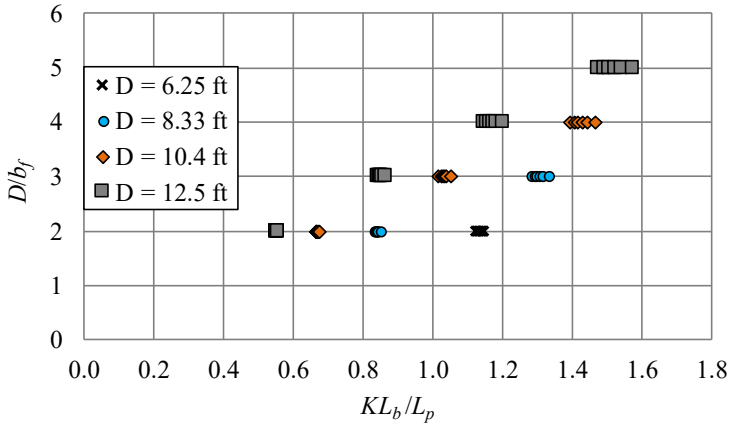

(c) $L_b/R = 0.10$

Figure 1: KL_b/L_p versus D/b_f for different web depths, D, and subtended angles, L_b/R, when the cross-frame spacing is at the maximum limit of $L_b = 30$ ft

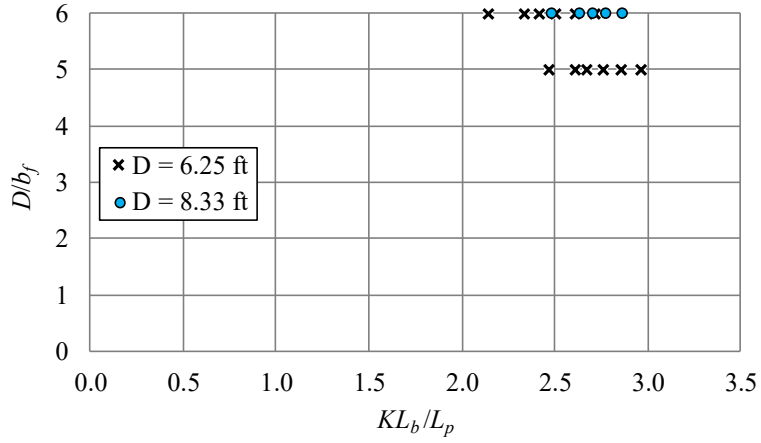

(a) $L_b/R = 0.05$

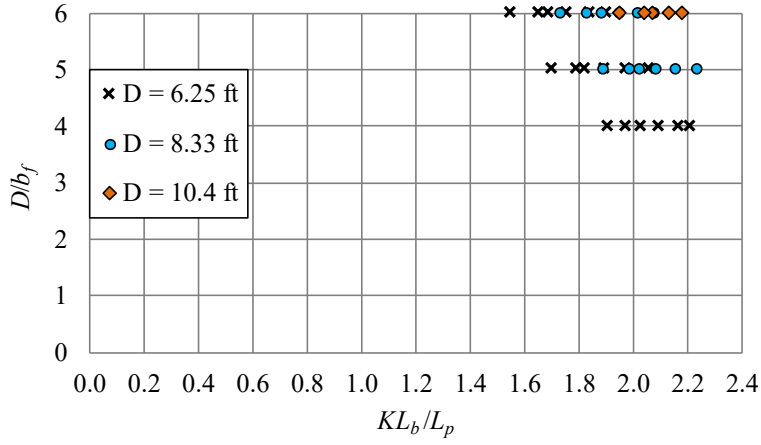

(b) $L_b/R = 0.075$

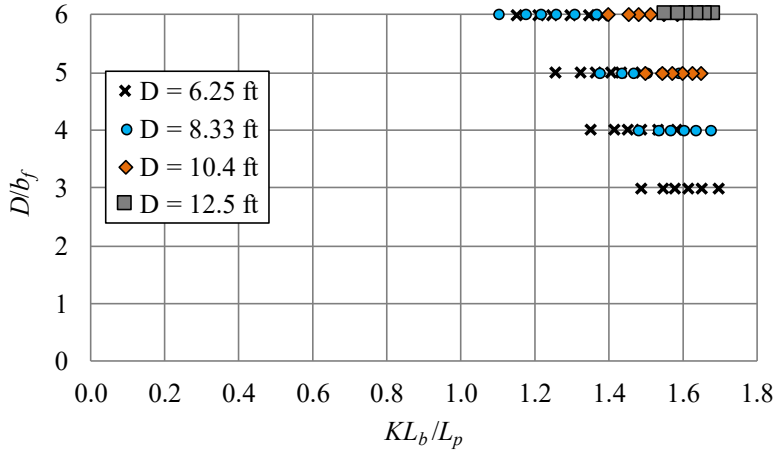

(c) $L_b/R = 0.10$

Figure 2: KL_b/L_p versus D/b_f for different web depths, D, and subtended angles, L_b/R, when the cross-frame spacing is less than 30 ft (limited by, $f_l/F_y = 0.6$)

2. When $D/b_f \geq 3$ in girders with smaller web depths (D = 6.25 ft) and larger curvatures (L_b/R = 0.1), $f_l = 0.6F_y$ controls in all cases, and thus the girders cannot be designed with L_b = 30 ft.
3. For cases where L_b = 30 ft governs, the maximum allowable values of KL_b/L_p are unaffected by the curvature. However, for cases governed by the $f_l = 0.6F_y$ limit, the maximum allowable values of KL_b/L_p decrease with increasing curvature. Furthermore, girders with larger D/b_f generally have larger flange lateral bending and are more sensitive to changes in the curvature. Therefore, for larger D/b_f, more of the girders are governed by the $f_l = 0.6F_y$ limit and thus show up in Fig. 2 rather than Fig. 1.
4. By comparing Figs. 1 and 2, one can observe that the largest values of KL_b/L_p are obtained when the limit on $f_l = 0.6F_y$ controls the design rather than the limit of L_b = 30 ft.
5. The design of horizontally curved longitudinally stiffened I-girders with D = 12.5 ft (or larger by inference) is restricted to values of KL_b/L_p of 2 or less. For girders with D = 12.5 ft and $D/b_f \leq 3$, the design is always governed by the LTB plateau region.
6. The girders with D = 10.4 ft never have KL_b/L_p larger than 2.5. For $D/b_f \leq 2$, these girders always fall within the plateau region of the LTB curve.
7. Girders with D = 8.33 ft, and 6.25 ft never have KL_b/L_p larger than 3. Girders with D = 8.33 ft tend to have KL_b close to the limiting plateau length L_p when $D/b_f = 2$. Girders with web depths of 6.25 ft always fall in the inelastic LTB region even for sections with $D/b_f = 2$.
8. For girders having cross-sections of similar proportions, girders with larger web depths have larger values of L_p than girders with smaller D. However, the cross-frame spacing is limited to 30 ft by the current AASHTO provisions. Hence, girders with larger D are necessarily restricted to smaller maximum KL_b/L_p values. This leads to a significant dependency of the permissible girder design space on the web depth rather than on normalized cross-sectional design parameters such as D/t_w.
9. For a given web depth, smaller values for the maximum permissible KL_b/L_p are attained for narrower flanges (larger D/b_f) when $f_l = 0.6F_y$ controls. This is because the narrower flange girders tend to attain a larger f_l for a given unbraced length (KL_b). This trend is reversed when L_b = 30 ft controls the design, i.e., smaller values of the maximum KL_b/L_p are attained for wider flanges (smaller D/b_f) for a given web depth. This is because the maximum KL_b is a constant for these girders, but the L_p values are larger for the girders with smaller D/b_f.

Figure 3 shows the f_l/F_y values in girders designed at the maximum unbraced length limit L_b = 30 ft. This figure shows the variation in the maximum f_l/F_y values versus D/b_f for different web depths, D, and subtended angles, L_b/R, for these girders.

The following can be gleaned from Figure 3:
1. For a given web depth, the flange lateral bending stresses increase with increasing D/b_f.
2. For a given D/b_f, the flange lateral bending stresses are larger for girders with smaller web depth. This is because the cross-frame spacing in these plots is constant at L_b = 30 ft. For a given unbraced length, smaller girder depths D result in larger flange lateral bending and greater stability effects, given other similar girder cross-section characteristics.

Figure 4 shows the combinations of D/b_f and D that yield $f_l = 0.6F_y$ for different subtended angles, L_b/R, from the above studies. The underlying values of L_b in this figure are smaller than the maximum allowable spacing of 30 ft.

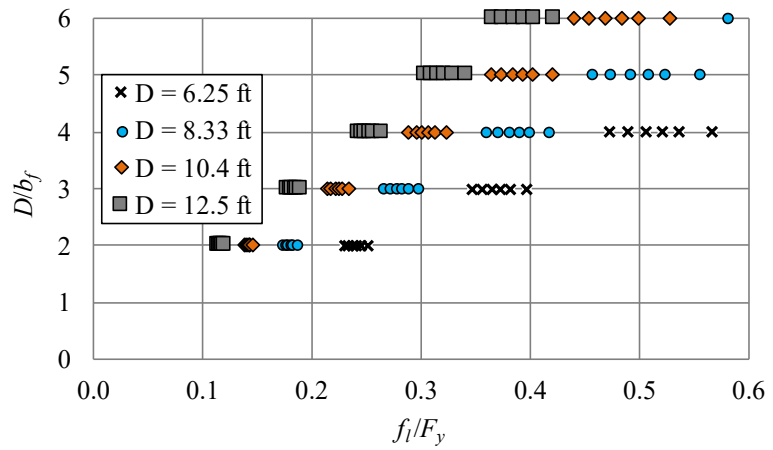

(a) $L_b/R = 0.05$

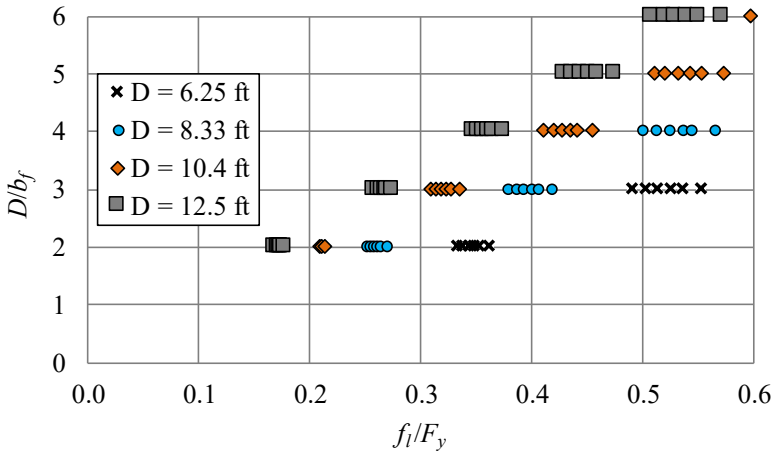

(b) $L_b/R = 0.075$

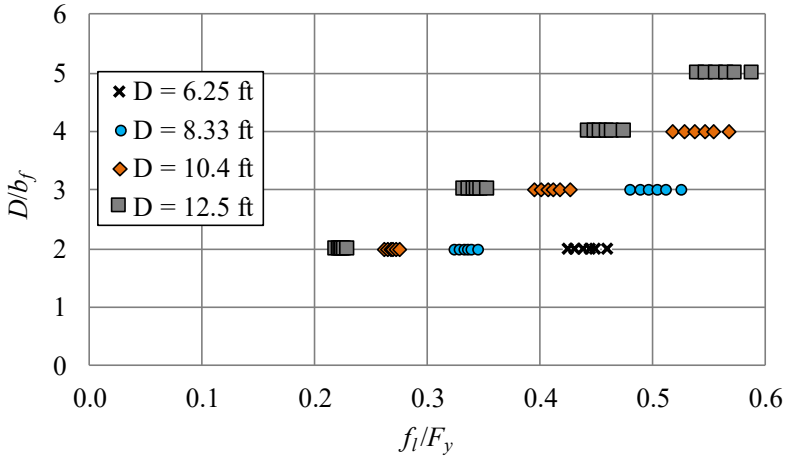

(c) $L_b/R = 0.10$

Figure 3: f_l/F_y versus D/b_f for different web depths, D, and subtended angles, L_b/R, for girders designed at the maximum unbraced length limit of $L_b = 30$ ft

Figure 4 complements and synthesizes the findings illustrated in Figs. 1 to 3. As would be expected, an increase in curvature (i.e., larger L_b/R) necessitates the use of wider flanges for a given web depth, in order to limit the flange lateral bending to a particular value. Conversely, to maximize the cross-frame spacing at a given curvature and D/b_f, a cross-section with larger web depth needs to be selected. To limit the flange lateral bending to a particular value, cross-sections with smaller web depth must necessarily have wider flanges for a given L_b or L_b/R. Cross-sections with larger depth may be designed with larger D/b_f for a given L_b or L_b/R.

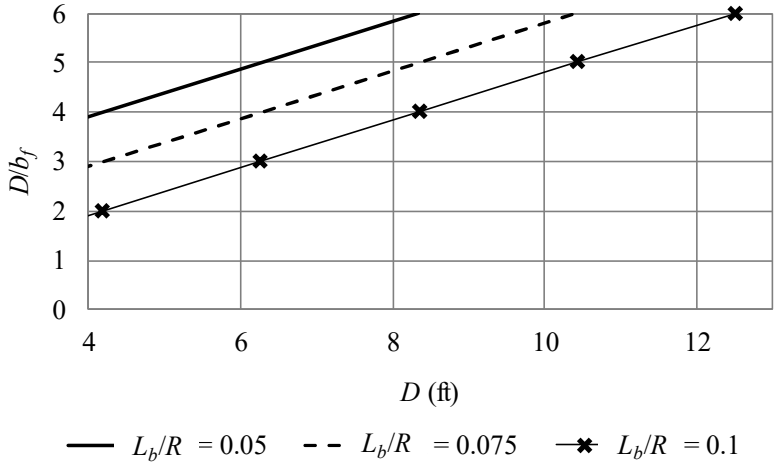

Figure 4: Values of D/b_f vs. web depth beyond which the cross-frame spacing L_b must be smaller than 30 ft to limit f_l to $0.6F_y$

3. Validation of One-Third Rule Using Finite Element Analyses

The test members used to validate the one-third rule in this section fail either by the LTB plateau limit state or by inelastic LTB, as explained in Section 2.4. The one-third rule is used along with proposed R_b from Eq. (1).

3.1 Test Members

To evaluate the applicability of the one-third rule for curved longitudinally-stiffened members, the most critical of such members are identified. The girders considered in this Section are designed to have relatively high flange lateral bending stresses within the limit of $0.6F_{yc}$ specified by the AASHTO LRFD Specifications.

The test members are selected with two different panel aspect ratios (d_o/D = 1, 2), with narrow and wide flanges encompassing three different web depths to thickness ratios. A total of 24 members are grouped into four categories as shown in Table 1.

Table 1: Case studies for horizontally curved longitudinally stiffened I-girders

Case	D (in)	D/b_f	L_b (ft)	L_b/R	d_o/D	D/t_w
1	150	3	30	0.11	1	200, 240, 300
2	150	6	30	0.05	1	200, 240, 300
3	75	3	30	0.07	2	150
4	75	6	17.875	0.03	2	150

For each of the cases, girders are considered with the longitudinal stiffener placed on the side of the web opposite from as well as toward the center of curvature, making the total number of tested girders 48. The difference in the designs with the longitudinal stiffener on the different sides of the web comes from the longitudinal stiffener rigidity requirements summarized in Section 2.1. Generally, AASHTO requires a slightly larger stiffener when the stiffener is placed on the side of the web opposite from the center of curvature. The prior studies by (Subramanian and White 2017d) found only a slight increase in the girder capacities with the stiffener placed on the outside compared to on the inside of the curve, and attributed this increase primarily to the larger size stiffener employed when the stiffener is on the outside. In this paper, the longitudinal stiffener is sized such that both the maximum b_l/t_s and the minimum I_l as required by AASHTO (2016) are simultaneously satisfied. The longitudinal stiffener is placed at the optimum depth for flexure ($0.4D_c$) from the inside of the compression flange (Dubas 1948). The transverse stiffener size (12.5 x 1.8 in) is selected such that the minimum AASHTO requirements are satisfied in all cases. The transverse stiffeners are assumed to remain elastic in all the test simulations.

In each of the four case studies, three values for the web depth in compression (D_c/D) are considered. The compression and tension flanges are taken to be of equal width in all the studies. The tension flange thicknesses are varied such that D_c/D = 0.5, 0.625 and 0.75. The compression flange thickness is selected such that $b_{fc}/2t_{fc}$ is 9, making the compression flange compact. It is shown in (Subramanian and White 2017e) that the flange local buckling equations in AASHTO (2016) are conservative for noncompact flanges, and that there appears to be no significant interaction between FLB and LTB for girders designed according to the AASHTO requirements. Moreover, as shown in Section 2.4, the use of noncompact flanges versus compact flanges does not have a significant influence on the maximum allowable L_b values.
Only homogeneous girders are considered in this study. Prior research by the authors has shown that early web yielding in hybrid girders has a negligible impact on the stability of the compression flange. The authors do not expect that a lower strength web will affect the validity of the one-third rule for curved longitudinally stiffened I-girders.

The cross-section and member parameters for the individual girder tests are listed in Table 2. The girders in Cases 1 and 2 have web depths of 150 in, while the girders in Cases 3 and 4 have web depths of 75 inches. Cases 3 and 4 are designed with smaller web depths for three reasons:

1. Members with smaller cross-sectional dimensions have a smaller L_p. This allows the study of girders with KL_b/L_p maximized, which helps analyze the behavior of girders failing by inelastic LTB. The values of KL_b/L_p are shown in Table 2.
2. The study of girders with d_o/D of 2 is possible when the web depths are smaller. The cross-frame spacing limit of 30 ft restricts the panel aspect ratios that can be studied for larger web-depth members. The study of girders with larger d_o/D also requires the use of smaller curvatures (Subramanian and White 2017d).
3. Girders with smaller web depths also attain larger flange lateral bending stresses, compared to girders with larger web depths as shown in Section 2.4. This allows the validation of the one-third rule for members with the largest possible flange lateral bending stresses.

The smallest web depth for a longitudinally stiffened girder, 75 in., is employed for Cases 3 and 4 (obtained using web longitudinal stiffeners on girders with D/t_w of 150, and taking the minimum practical bridge girder web thickness as 0.5 in).

Table 2: Test girder cross-section and member properties

Case	Girder	D/t_w	D_c/D	R_{bPr}	$R_{bAASHTO}$	Z	KL_b/L_{br}
	G1	300	0.500	1.00	0.94	12.95	0.86
	G2	240	0.500	1.00	1.00	10.36	0.87
	G3	200	0.500	1.00	1.00	8.64	0.88
	G4	300	0.625	0.98	0.89	12.95	0.87
1	G5	240	0.625	0.99	0.91	10.36	0.88
	G6	200	0.625	1.00	1.00	8.64	0.89
	G7	300	0.750	0.96	0.82	12.95	0.88
	G8	240	0.750	0.96	0.85	10.36	0.89
	G9	200	0.750	0.97	0.87	8.64	0.90
	G10	300	0.500	0.96	0.81	5.94	1.92
	G11	240	0.500	0.99	1.00	4.75	1.98
	G12	200	0.500	1.00	1.00	3.96	2.04
	G13	300	0.625	0.90	0.68	5.94	1.98
2	G14	240	0.625	0.93	0.75	4.75	2.05
	G15	200	0.625	0.98	1.00	3.96	2.12
	G16	300	0.750	0.85	0.54	5.94	2.04
	G17	240	0.750	0.88	0.63	4.75	2.12
	G18	200	0.750	0.91	0.70	3.96	2.21
	G19	150	0.500	1	1	8.48	1.78
3	G20	150	0.625	1	1	8.48	1.82
	G21	150	0.750	1	1	8.48	1.85
	G22	150	0.500	1	1	6.48	2.57
4	G23	150	0.625	1	1	6.48	2.70
	G24	150	0.750	1	1	6.48	2.83

3.2 Test Setup

All the tests in this study are four-point bending configurations with the test specimen inserted within the length subjected to uniform bending and flanked by an end fixture on each side (see Fig. 5). The end fixtures are designed to develop the strength of all the test specimens. The web and flange plates in the end fixtures are significantly thicker (2 to 3 times thicker) than the plates used in the test specimens. This setup is similar to that used in the straight girder studies in (Subramanian and White 2017d). The fixtures are restrained torsionally and laterally at the end vertical supports, as indicated by the X symbols in the figure. In addition, the girders are restrained torsionally and laterally at the points of application of the external vertical loads, and at the ends of the test specimen. The end fixtures are straight. The curved test specimen is tangential to the end fixtures at the point of transition. Large stiff curved end fixtures would induce large radial bracing forces; the end fixtures are designed as straight components to avoid this issue.

It is essential to use the correct effective length factor for the computations discussed in this research. In general, this is the only meaningful way that LTB test results can be compared to LTB strength predictions. Without consideration of end restraint effects via an effective length factor, the correlation between I-girder LTB strength predictions and test results generally will be poor.
Within the test setup shown in Fig. 5, the test specimen is an essential component in resisting the applied loads. The predominant loading of the test specimens is uniform major-axis bending.

Warping of the flanges is essentially fully restrained at the ends of the test specimens, and in addition, the flange lateral bending rotations are essentially zero at test specimen ends.

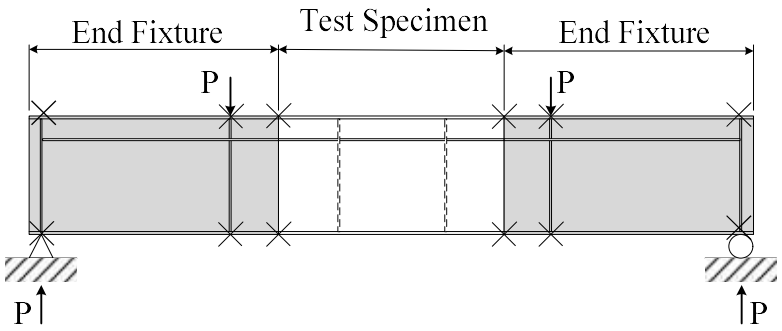

Figure 5: Test setup for uniform bending

The failure mode of the test specimen in all these cases involves lateral movement of the compression flange in the direction away from the center of curvature, with the flange lateral bending rotations being essentially fixed at the connection to the end fixtures. The best approximation of this behavior for the purposes of design calculation using the AASHTO LRFD resistance equations is with an effective length of $0.5L_b$, where L_b is the test specimen length. Therefore, $K = 0.5$ is used in all the following studies in this paper.

3.3. Finite Element Modeling

In this research, full nonlinear analyses are conducted to simulate physical tests using ABAQUS (Simulia 2013). The finite element modeling parameters, including the discussion on geometric imperfections and residual stresses is given in (Subramanian and White 2016a).

3.4 Stress Calculations

The values of the elastically calculated flange lateral bending stresses (f_l) and compression flange major-axis bending stresses (f_{bu}) are used in the discussion of the test results. An explanation of how these terms are computed, both from FEA results and by manual estimates is provided below.

3.4.1 Calculation of Stresses from FEA

The stresses reported as being obtained directly from FEA are calculated using the procedure from (White et al. 2001). In this procedure, , the analyses are performed for the same loads as in the full nonlinear analysis test simulations, but the material is taken to be completely elastic for the purpose of the design resistance calculations. This includes any effects of elastic web distortion and/or elastic web buckling on the compression flange stresses. Since the analysis is geometrically nonlinear, the stresses computed by the following method are second-order elastic stresses, and no separate amplification is required. The procedure for the calculation of the elastic design stresses is as follows:

1. The stresses in the shell elements are extrapolated to the tips of the flanges at the location of the maximum flange lateral bending.
2. The major-axis bending stress, f_{bu} is calculated as the average of the two flange tip stresses.
3. The flange lateral bending stress, f_l is calculated as one-half the difference between the two flange tip stresses. The compression flange experiences larger flange lateral bending stress than the tension flange, and it is this value that is used in the one-third rule resistance checks.

The full nonlinear analysis test simulation is first performed on each test girder. A second elastic geometrically nonlinear analysis is then carried out, with the load set to the peak load obtained from the first analysis. The elastic stresses, f_{bu} and f_l are calculated at the peak load from this second FE model using the method described above. Geometric imperfections are not included in the elastic analysis. These values are reported with the subscript "FEA" in the subsequent discussions.

3.4.2 Manual Calculation of Stresses

The major-axis bending stress, f_{bu} is calculated as M_{max}/S_{xc}, where M_{max} is the maximum major-axis bending moment attained by the girder in the full nonlinear analysis, and S_{xc} is the elastic section modulus to the girder compression flange, including the contribution of the longitudinal stiffener. The horizontal curvature of the girder results in major-axis bending (about the radial axis), and twisting about the tangential axis of the girder. However, the total subtended angle between the end vertical supports due to horizontal curvature considered in these studies is small (≤ 0.11 radians). For such members, it is a reasonable simplification to approximate the major-axis bending moment in the horizontally curved beam as the applied bending moment at the ends of the test specimen. The influence of the eccentricity of the single-sided longitudinal stiffener on the cross-section principal axis is neglected.

The elastic second-order flange lateral bending stress, f_l, is calculated as the product of the first-order stress from Eq. (13) and the amplification factor of Eq. (14). In Eq. (12), the moment M is taken as the major-axis bending moment in the test specimen at the strength limit of the full nonlinear test simulation, and N is taken as 12. The values calculated by the above manual procedure are reported with the subscript "DS".

3.5 Synthesis of Results

This section discusses the validity of the one-third rule for curved longitudinally stiffened girders. Subramanian and White (2017f) discuss that there is no distinct advantage of placing the stiffener on one side of the web versus the other. Table 3 provides the values of the elastic design stresses calculated manually and directly from FEA for the 24 test girders, as well as the result from their substitution into the one-third rule. The following may be gleaned from these tables:

1. The manually calculated elastic flange lateral bending stresses, f_l, are always conservative relative to the stresses calculated from FEA. Similarly, the elastic major-axis bending stresses computed as M_{max}/S_{xc} are larger than the stresses computed from the FEA. The over-estimation of the theoretical flange lateral bending stresses is due to the conservative nature of the manual equations for f_l. The applied load causes both major-axis bending and twist (accompanied by flange lateral bending). However, the manual calculation of the major-axis bending stresses neglects the effect of the twist rotation, and hence slightly over-estimates the true major-axis bending stresses.
2. The smallest values of the flange lateral bending stresses are achieved by the girders in Case 1, which have deeper web depths (D = 150 in) and wide flanges (D/b_{fc} = 3) despite having a larger subtended angle (L_b/R = 0.11). The largest values of the flange lateral bending stresses are achieved by the girders in Case 4, which have the smallest web depths (D = 75 in), narrow flanges (D/b_{fc} = 6) and the smallest subtended angle (L_b/R = 0.045). It is worth noting that the flange lateral bending stresses for the Case 4 girders (G22 to G24) are larger than those for the Case 1 girders (G1 to G9) even though the Case 1 girders have a larger L_b/R. This combined effect of small web depths and narrow flanges is also evident in Figs. 1 and 2.

Table 3: Peak load and elastic design stresses for girders with longitudinal stiffener placed on the side of the web toward the center of curvature

Girder	$f_l/F_{yc\text{DS}}$	$f_l/F_{yc\text{FEA}}$	$f_{bu}/F_{yc\text{DS}}$	$f_{bu}/F_{yc\text{FEA}}$	F_{ncPr}/F_{yc}	$(f_{bu}+1/3f_l)_{\text{DS}}/F_{ncPr}$	$(f_{bu}+1/3f_l)_{\text{FEA}}/F_{ncPr}$
G1	0.43	0.30	0.91	0.83	1.00	1.04	0.93
G2	0.44	0.31	0.92	0.84	1.00	1.06	0.94
G3	0.45	0.32	0.94	0.85	1.00	1.08	0.96
G4	0.43	0.30	0.89	0.82	0.98	1.04	0.94
G5	0.45	0.31	0.90	0.82	0.99	1.05	0.94
G6	0.47	0.30	0.92	0.83	1.00	1.06	0.93
G7	0.43	0.30	0.87	0.81	0.96	1.05	0.95
G8	0.45	0.31	0.88	0.81	0.96	1.06	0.95
G9	0.47	0.33	0.90	0.82	0.97	1.07	0.95
G10	0.44	0.37	0.83	0.68	0.89	1.09	0.90
G11	0.49	0.41	0.86	0.71	0.91	1.11	0.93
G12	0.52	0.43	0.88	0.73	0.91	1.14	0.96
G13	0.46	0.38	0.77	0.64	0.83	1.10	0.93
G14	0.51	0.42	0.81	0.67	0.85	1.14	0.96
G15	0.58	0.46	0.83	0.70	0.89	1.14	0.96
G16	0.46	0.37	0.74	0.63	0.78	1.14	0.98
G17	0.52	0.42	0.76	0.64	0.80	1.17	0.98
G18	0.58	0.47	0.80	0.68	0.82	1.21	1.02
G19	0.60	0.49	0.89	0.76	0.94	1.15	0.99
G20	0.63	0.51	0.89	0.76	0.93	1.17	1.00
G21	0.66	0.50	0.89	0.75	0.93	1.18	0.99
G22	0.51	0.44	1.05	0.78	0.87	1.43	1.07
G23	0.59	0.55	1.10	0.83	0.86	1.56	1.18
G24	0.65	0.58	1.04	0.78	0.85	1.52	1.14
Mean	0.51	0.40				1.16	0.98
COV	0.15	0.22				0.12	0.07
Min	0.43	0.30				1.04	0.90
Max	0.66	0.58				1.56	1.18
Median	0.48	0.39				1.12	0.96

3. The equivalent compression flange design stress, $(f_{bu}+1/3f_l)_{\text{FEA}}$ is smaller than the design strength F_{nc} for all of Case 1 girders (G1 to G9), and some of the girders in Case 2 (G10 to G18). The largest strength ratios are attained by the girders in Case 4 (G21 to G24). The most unconservative value of the strength ratio is 0.91, and is attained by a girder with D = 150 in, D/b_{fc} = 3, KL_b/KL_p = 0.86 (plateau design strength), L_b/R = 0.11, and D/t_w = 300. Also, the most conservative value of the strength ratio is 1.18. This is attained by a girder with D = 75 in, D/b_{fc} = 6, KL_b/KL_p = 2.70 (inelastic LTB design strength), L_b/R = 0.03, and D/t_w = 150. This behavior stems from the following:
   a. Girders that have low values of KL_b/L_p tend to have a larger spread of plasticity within the cross-section at the strength limit. In such girders, flange lateral bending causes significant out-of-plane deformations leading to further loss of stability. This flange lateral bending effect is not captured by the design strength equation (F_{ncPr}), resulting in an over-estimation of the design strengths of such girders. Thus, the girders in Case 2 have larger strength

ratios than girders in Case 1, and the girders in Case 4 have larger strength ratios than the girders in Case 3.

b. The girders in Cases 3 and 4 are designed with panel aspect ratios of 2.0. These girders have relatively large longitudinal stiffeners (as per AASHTO requirements), which contribute to larger strength ratios for these girders.

4. The coefficient of variation (COV) of $(f_{bu}+1/3f_l)_{FEA}$ is much smaller than the COV of $(f_{bu}+1/3f_l)_{DS}$. In addition, $(f_{bu}+1/3f_l)_{DS}$ is significantly more conservative than $(f_{bu}+1/3f_l)_{FEA}$. This is largely due to the conservative approximations in the calculation of the flange lateral bending stresses using the AASHTO design equations discussed in Section 2.2.

4. Conclusions

The principal findings in this paper are summarized below:

1. The design of curved longitudinally-stiffened I-girders always fall within the LTB plateau or the shorter lengths of the inelastic LTB region.
2. The recommendations for straight longitudinally stiffened girders also provide an improvement over the current LRFD equations for curved longitudinally-stiffened girders, both in terms of the strength predictions, as well as the overall scatter of data. The one-third rule when used along with the current equations (AASHTO 2016) are clearly conservative. The one-third rule along with the proposed equations (modified R_b and modified LTB equations) work reasonably well (mean of 0.98 and COV of 0.07 for $(f_{bu}+1/3f_l)_{FEA}$ as compared to a mean of 1.16 and a COV of 0.12 for $(f_{bu}+1/3f_l)_{DS}$ for longitudinal stiffeners placed on the side of the web toward the center of the curvature). This accuracy is acceptable for design.
3. Lastly, the paper also shows that values of Z up to 13 can be safely used in design.

References

AASHTO (2016). *AASHTO LRFD Bridge Design Specifications. 7th Edition with Interim Revisions*, American Association of State Highway and Transportation Officials, Washington, DC.

Dubas, C. (1948). "Contribution A` L' E'tude Du Voilement Des To`les Raidies (A Contribution to the Buckling of Stiffened Plates)."

Simpson, M. D. (2000). "Analytical Investigation of Curved Steel Girder."Doctoral Dissertation, Doctoral Dissertation, University of Toronto, Toronto, CA.

Simulia (2013). *ABAQUS/Standard Version 6.12-1*, Simulia, Inc, Providence, RI.

Subramanian, L. P., and White, D. W. (2017a). "Flexural Resistance of Longitudinally Stiffened I-Girders. I: Yield Limit State." *Journal of Bridge Engineering*, 22(1).

Subramanian, L. P., and White, D. W. (2017b). "Improved Strength Reduction Factors for Steel Girders with Longitudinally Stiffened Webs." *Structural Engineering, Mechanics and Materials Report No. 112*, School of Civil and Environmental Engineering, Georgia Institute of Technology, Atlanta, GA.

Subramanian, L. P., and White, D. W. (2017c). "Flexural Resistance of Longitudinally Stiffened I-Girders. II: LTB and FLB Limit States." *Journal of Bridge Engineering*, 22(1).

Subramanian, L. P., and White, D. W. (2017d). *Flexural Resistance of Longitudinally Stiffened Plate Girders*, Updated Report to AASHTO and AISI, School of Civil and Environmental Engineering, Georgia Institute of Technology, Atlanta, GA.

Subramanian, L. P., and White, D. W. (2017e). "Reassessment of the Lateral Torsional Buckling Resistance of I-Section Members : Uniform Moment Studies." *Journal of Structural Engineering, ASCE*, 143(3).

Subramanian, L. P., and White, D. W. (2017f). *Flexural Resistance of Longitudinally Stiffened Curved I-Girders*, Report to AASHTO and AISI, School of Civil and Environmental Engineering, Georgia Institute of Technology, Atlanta, GA.

White, D. W., Zureick, A. H., Phoawanich, N. P., and Jung, S.-K. (2001). "Development of Unified Equations for Design of Curved and Straight Steel Bridge I-Girders." *Final Report to AISI, PSI, Inc. and FHWA,*.

White, D. W., and Grubb, M. A. (2005). "Unified Resistance for Design of Curved and Tangent Steel Bridge I-Girders." *TRB 6th International Bridge Engineeering Conference*, Transportation research Board, 20pp.